Available online at www.sciencedirect.com
SCIENCE DIRECT®
Catalysis Today 107–108 (2005) 458–466
CATALYSIS TODAY
www.elsevier.com/locate/cattod

Naphtha steam reforming for hydrogen production

F. Melo *, N. Morlanés

Instituto de Tecnología Química, UPV-CSIC, Avda. los Naranjos s/n, 46022 Valencia, Spain

Available online 16 August 2005

Abstract

A study based on hydrogen production by catalytic naphtha steam reforming is presented. Reaction product composition depends on process conditions, which govern the equilibrium of gas species. This study has been realized in a fixed-bed-type reactor with a commercial steam reforming nickel catalyst and with a series of catalysts obtained by thermal decomposition of nickel based hydrotalcites. Operation condition influence has been studied. Catalysts prepared from hydrotalcites are promising materials to use in steam reforming reactions, since their catalytic activity is significantly higher than it is for the commercial one. These samples have been characterized by various techniques in order to correlate their activity with their structural characteristics. Finally, we have determined how the nickel content of hydrotalcite-derived catalysts affects their catalytic activity and resistance to carbon formation for naphtha steam reforming reaction.
© 2005 Elsevier B.V. All rights reserved.

Keywords: Steam reforming; Hydrogen production; Naphtha; Hydrotalcite-materials

1. Introduction

Hydrocarbon steam reforming is an important process for hydrogen production. Hydrogen is a valuable raw material for chemical and petrochemical industry and it is also used as a clean combustible. Other techniques for hydrogen production are partial oxidation and autothermal reforming. From the point of view of hydrogen application as fuel for fuel cells, hydrocarbon steam reforming is the technology producing the highest hydrogen concentration on the effluent [1]. Nevertheless, endothermic nature of this reaction requires great energy contribution, so thermal integration of hydrocarbon reforming process with operation of electrochemical cell is essential to reach high effectiveness of the global process [2]. On the other hand, in the case of mobile fuel cell applications, liquid hydrocarbon use benefits from the infrastructure already created for fuel storage and distribution [3]. Optimal election of the most suitable technology and the best hydrocarbon type for hydrogen production depends on the final product application, which determines gas composition requirements and operation scale [4].

Steam reforming process transforms a liquid hydrocarbon stream into a gaseous mixture constituted by CO_2, CO, CH_4, and H_2. The main reactions that take place are the following ones [5]:

$$C_nH_m + nH_2O \rightarrow nCO + (n+\tfrac{1}{2}m)\,H_2 \quad \Delta H < 0 \tag{1}$$

$$CO + 3H_2 \leftrightarrow CH_4 + H_2O \quad \Delta H = -206\,\mathrm{kJ/mol} \tag{2}$$

$$CO + H_2O \leftrightarrow CO_2 + H_2 \quad \Delta H = -41.2\,\mathrm{kJ/mol} \tag{3}$$

Total hydrocarbon conversion is achieved in a usual practice of this process, so that the reaction product composition is determined by the thermodynamic equilibrium between gaseous species according to operation conditions at which this process takes place (pressure, temperature, steam/carbon ratio and space velocity) [5]. Thus, for producing a hydrogen-rich gas effluent is suitable working at low pressure, high temperature and with a high steam/carbon ratio, with the purpose of moving the thermodynamic equilibrium, which determines the composition of the gas, towards hydrogen formation.

Steam reforming reaction takes place on the surface of a solid catalyst. For this process usually nickel based catalysts are used, this metal presents a good activity/cost ratio, nickel is supported on a material that confers its sufficient

* Corresponding author. Tel.: +34 96 387 78 10; fax: +34 96 387 78 09.
E-mail address: fmelo@itq.upv.es (F. Melo).

0920-5861/$ – see front matter © 2005 Elsevier B.V. All rights reserved.
doi:10.1016/j.cattod.2005.07.028

mechanical and thermal resistance for the process, being normally used aluminium oxide with additives that prevent carbon formation. Alkali addition (KO_2) and basic supports use (MgO) is common for this aim [5].

Reaction mechanism, proposed by Rostrup Nielsen [5,6], establishes that hydrocarbon molecules are adsorbed on catalyst surface where nickel selectively attacks terminal carbon of the chain by means of successive α-scission steps. Resulting C_1 species formed can react with oxygen species coming from water adsorption-dissociation, or remain adsorbed on the active sites where they would be transformed according to one of the possible carbon formation routes. We can outline this sequence:

Hydrocarbon adsorption-dissociation:

$$C_nH_m + 2* \rightarrow C_nH_z\cdots *2 + \frac{m-z}{2}H_2 \quad (4)$$

C–C α-scission:

$$C_nH_z\cdots *2 + n* \rightarrow C_{n-1}H_z'\cdots *2 + CH_x\cdots *n \quad (5)$$

Steam adsorption-dissociation:

$$H_2O + * \rightarrow O\cdots * + H_2 \quad (6)$$

CH_x--*n + O--* → CO + x/2 H_2 + (n+1)* (*gasification*) (7)

CH_x--*n → [Ni, C] →" whisker" (*whisker carbon*) (8)

C--* →"gum" (*gum carbon*) (9)

Therefore, carbon formation, which is the main disadvantage of steam reforming process, is a kinetic question; it will depend on the relative rate of the possible C_1 species reaction alternatives [7,8]. Process could take place through a mechanism or another one and it will depend on hydrocarbon type, operation conditions, and catalyst characteristics, which can play an important role in increasing selectivity towards the preferred reaction.

Catalyst characteristics can influence [6] by increasing:

- Water adsorption–dissociation rate on the catalyst.
- Gasification rate with respect to the C–C scission.

Due to severe operation conditions at which the process normally takes place, in addition to the carbon formation, other deactivation mechanisms can act. The most important ones are sintering of metallic nickel, which entails coalescence of metal particles [9,10] and reduction of active surface area, oxidation of metallic nickel [5,6] and nickel-support reaction forming hardly reducible compounds (as $NiAl_2O_4$) [11]. The measurement in which these deactivation mechanisms could also occur will depend on catalyst characteristics, hydrocarbon type, and operation conditions.

Due to these disadvantages, a good steam reforming catalyst must have the following characteristics [6]:

- High mechanical resistance.
- High thermal stability.
- High resistance to carbon formation.
- High catalytic activity.
- High selectivity towards hydrocarbon gasification.

Catalyst characteristics are determined by their physical chemistry, structural and textural properties, as they are: active area, metal particle size, metal dispersion and reducibility, etc. These properties depend on metal-support interaction, and they could be established on different stages of catalyst synthesis. For example, varying precursor material composition, preparation method, and/or heat treatments (calcination, reduction) [12–16].

Mixed oxides obtained by hydrotalcite-type material thermal decomposition [17,18] offer the opportunity to control the active site nature and its environment, as well as catalyst texture and stability. They can be prepared with different cations in its structure obtaining multifunctional material. Hydrotalcites containing noble or transition metals, after a suitable activation treatment, give rise to a metal supported catalyst type; metal-support interaction allows controlling metal particle size, and its stability. Mixed oxides derived from hydrotalcites present high activity, stability, and resistance to carbon formation [19,20].

In the present work, we have studied operation condition effect on reaction product composition for hydrocarbon steam reforming. Also, catalytic activity of a commercial catalyst was compared with that of a series of catalysts obtained by hydrotalcite-type materials thermal decomposition, and finally, nickel content effect on catalytic activity and on resistance to carbon formation has been determined.

2. Experimental

2.1. Catalytic system

Steam reforming reaction study is carried out in a fixed bed catalytic system designed for this purpose, which allows comparing different catalysts and reaction conditions, with the aim of optimising hydrogen production. The equipment is constituted by a tubular reactor inside a furnace. Liquid reactants (hydrocarbon and water) are pumped towards the reactor passing first through a pre-heater-evaporating zone; they arrive on gas phase at the reactor where they cross the catalytic bed reacting on the catalyst surface. Finally, gaseous flow that leaves the reactor (CO, CO_2, CH_4, H_2, H_2O and hydrocarbon) goes to a condenser, where water and hydrocarbon excess is separated, and reaction products are analysed by gas chromatography. The gas chromatograph is constituted by two independent channels, equipped each one of them with a thermal conductivity detector. First channel

allows separating CO_2, CO, CH_4, and N_2; and the second one allows to separate hydrogen from the rest of constituents.

Hydrocarbon feed is composed by a mixture of *n*-heptane and *n*-hexane (in a weight ratio of $C_7/C_6 = 2$) simulating a naphtha. Water and hydrocarbon feed are introduced mixed with a proportion of nitrogen and hydrogen. Nitrogen is used as carrier gas and as internal pattern for gas analysis. Hydrogen is used to avoid nickel oxidation in reduced samples.

Operation conditions studied are: P = 1–10 bar, T = 723–873 K, S/C = 3–6 H_2O mol/atom C, W/F = 1–8 g_{cat} h/hydrocarbon mol, $P_{H_2O}/P_{H_2} = 8$.

2.2. Catalyst preparation and characterization

As base catalyst, a commercial steam reforming catalyst constituted by nickel impregnated on an alumina–magnesia support has been used (Haldor–Topsoe R67-7H). This catalyst contains a 18% in weight of nickel, and its BET area is 23 m^2/g.

In order to determine nickel content effect on catalytic activity several catalysts based on nickel–magnesium–aluminium mixed oxides have been prepared, obtained by hydrotalcite type material thermal decomposition. These catalysts have been named with HT letters followed by a number, which indicates nominal nickel content (percentage in weight). Hydrotalcite type material synthesis is constituted by the following steps:

- Coprecipitation, on basic medium, those solutions containing the interest metals.
- Obtained gel crystallization (333 K).
- Washing the solid until neutral pH.
- Drying (333–353 K).

These materials have been calcined in air at 923 K during 8 h and then reduced, in situ, with hydrogen at 873 K during 15 h before being exposed to reaction mixture.

Solids, calcined and reduced samples, have been characterized by means of diverse techniques to try to correlate catalytic activity results with their structural properties. Techniques used for their characterization were:

- Atomic absorption spectroscopy, to know composition.
- X-rays diffraction, to know crystalline structure.
- Temperature programmed reduction, to know nickel reduction temperature.
- Nitrogen isothermal adsorption/desorption, to know BET area.

From diffraction patterns, crystalline phase particle size has been estimated using the greatest intensity diffraction signal, by means of Scherrer equation.

From temperature programmed reduction curves, temperature at which a maximum in the curve appears (nickel reduction temperature) has been used like a nickel-support interaction degree measurement.

Nickel area has been estimated by means of a proposed equation on literature [12–14] that considers nickel particle size, nickel content on the sample and reduction degree reached on the activation stage. The equation is the following one:

$$A_{Ni} = \frac{5 \times 10^4 X_{Ni} \alpha_{Ni}}{\gamma_{Ni} d_{Ni}} \quad (10)$$

where A_{Ni} is the nickel active area (m^2/g_{cat}); X_{Ni} the nickel content of the sample (g_{Ni}/g_{cat} %); A_{Ni} the reached reduction degree (g_{Ni0}/g_{Ni} %); g_{Ni} the nickel specific density, 8.9 g/cm^3; d_{Ni} the nickel particle size (Å); 5×10^4 is the geometric factor taking into account nickel particle geometry.

2.3. Activation stage optimisation

Catalyst activation stage is a metal reduction process, which initially is in the catalysts like oxide, this process requires a catalyst treatment with a reducing agent (hydrogen) at high temperature. With the purpose of determining optimal activation stage temperature, pressure, and duration, several reduction tests with one of the less reducible catalysts have been made. We have compared reached conversion at the same reaction conditions, making reduction stage in different ways (varying temperature, pressure or reduction time).

2.4. Catalytic activity

In order to determine operation condition effect on reaction product composition, two series of tests have been made using the same catalyst: first, varying contact time and fixing the rest of variables (pressure, temperature and steam/carbon ratio) to see how conversion degree affects thermodynamic equilibrium for gaseous species. Second, working with sufficiently long contact time to obtain total hydrocarbon conversion and to reach gases thermodynamic equilibrium, the rest of variables (temperature, pressure, steam/carbon ratio) have been modified to see their effect on the reaction product composition.

In order to compare catalytic activity for different catalysts, several tests have been made at the same operation conditions (pressure, temperature and steam/carbon ratio) and at sufficiently short contact time so that hydrocarbon conversion is not total, therefore the most active catalyst is this one that allows to reach the greatest conversion degree at the same time of reaction.

About catalytic activity tests, several observations have been made. Tests in which total hydrocarbon conversion has been reached, detected reaction products were CO, CO_2, CH_4, and H_2. Deactivation of the catalyst is not observed during the reaction time tested (5 h). On the other hand, tests in which only partial hydrocarbon conversion have been reached, activity drops gradually, more quickly whichever minor is the reached conversion degree, and for conversions smaller than 10%, C_2 traces could appear on the reaction

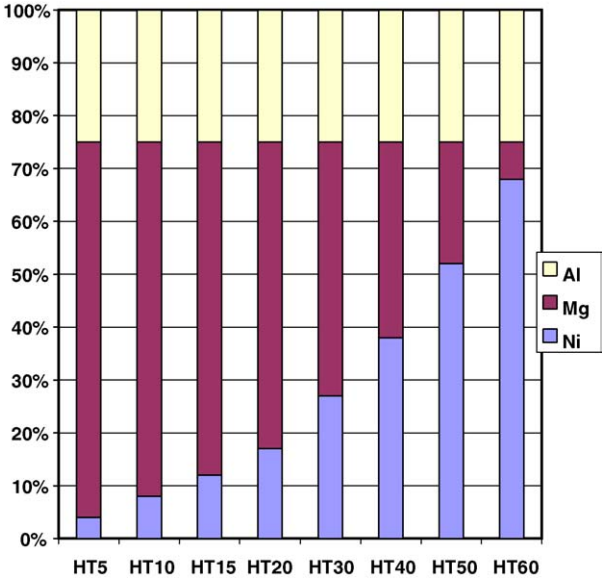

Fig. 1. Ni/Mg/Al molar proportion.

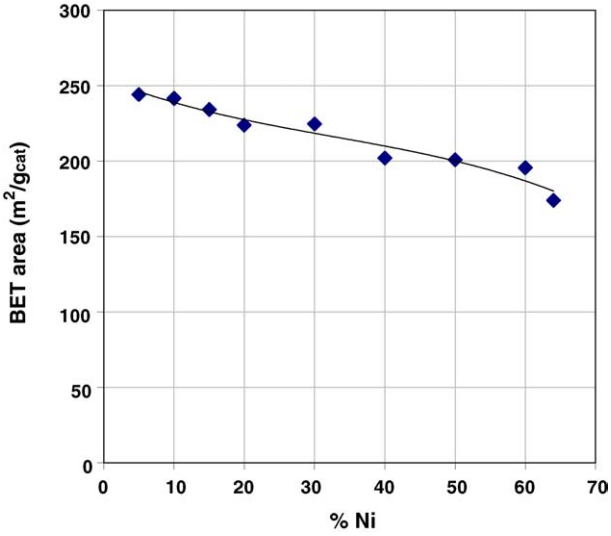

Fig. 3. BET area in function of nickel content.

products. In this case the activity measurement used to compare the behaviour for different catalysts corresponds to the reached conversion at the 45 min of reaction time, corresponding to the higher conversion observed.

2.5. Resistance to carbon formation

With the purpose of determining a relative measurement of resistance to carbon formation for different catalysts, a series of experiments at total hydrocarbon conversion has been made at the same operation conditions (pressure, temperature, contact time and steam/carbon ratio). During these tests, the steam/carbon ratio has been diminished, verifying carbon balance for each tested ratio. The limit steam/carbon ratio considered of each catalyst is that at which the carbon balance is smaller than 95%, that is to say, when less than 95% of fed carbon is recovered with gases at the exit of the reactor (as CO, CO_2 and CH_4), and therefore the rest is remaining adsorbed on the catalyst like coke or coke precursor.

3. Results and discussion

3.1. Catalyst preparation and characterization

It has been synthesized and characterized a series of catalysts with different nickel content, between 5 and 60% in weight. In Figs. 1–3 calcined samples characterization results appear.

In Fig. 1 we can see molar proportion of different compounds on synthesized samples obtained by atomic

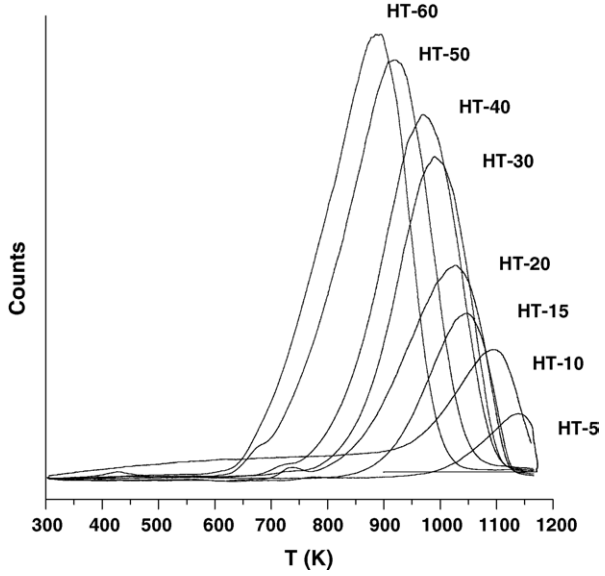

Fig. 2. Temperature programmed reduction (TPR).

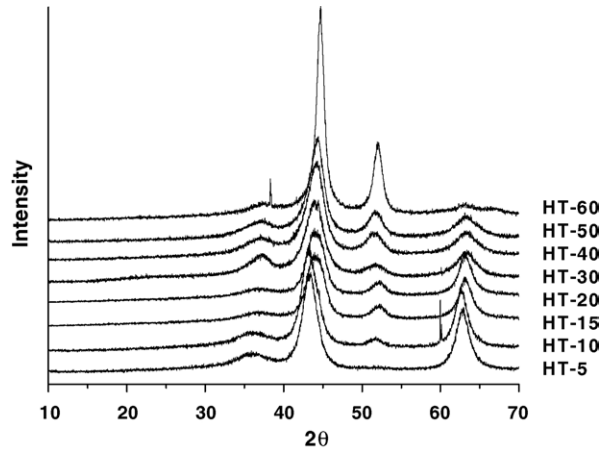

Fig. 4. X-ray diffraction of reduced samples.

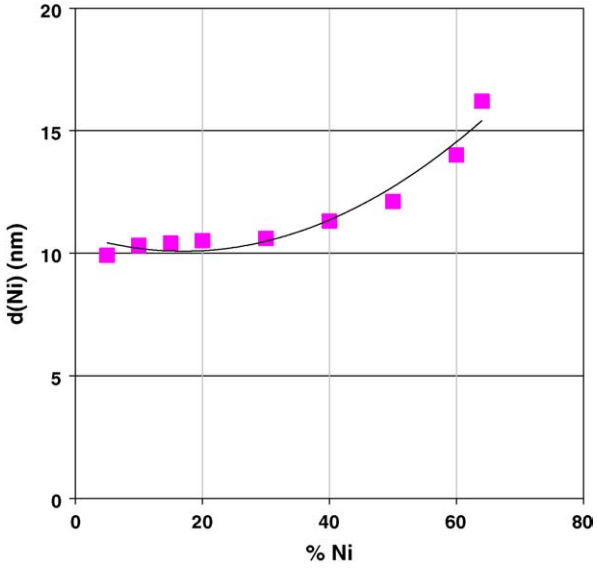

Fig. 5. Estimated nickel particle size vs. nickel content.

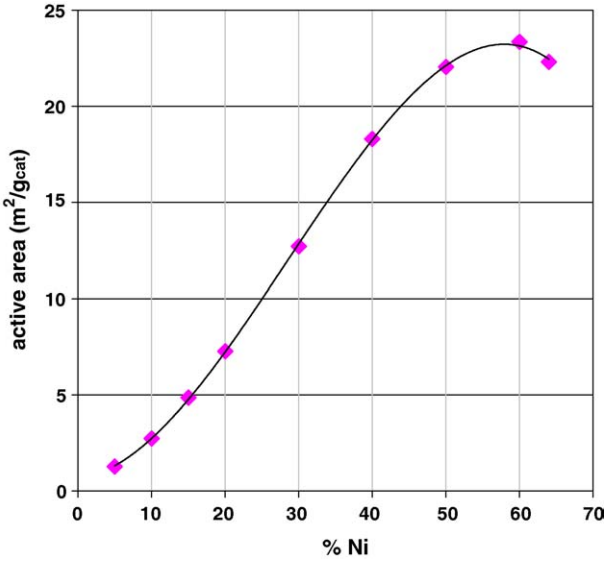

Fig. 7. Estimated nickel active area vs. nickel content.

absorption spectroscopy. In Fig. 2 we can see the curves of temperature programmed reduction, oxide is less reducible when nickel content decreases, this result gives us a qualitative measurement of nickel dispersion, since the most dispersed particles show stronger interaction with the support and usually they are less reducible. In Fig. 3 we can see that surface area diminishes as nickel content increases.

This series of catalysts also has been characterized after reduction treatment, characterization results are presented in Figs. 4–7.

In Fig. 4 we can see X-rays diffraction patterns corresponding to reduced samples. From these results, using diffraction signal corresponding to metallic nickel (band at $2\theta = 51^{\circ}$) we have estimated nickel particle size by means of Scherrer equation. In Fig. 5 we observe that nickel particle size increases with nickel content, in the same sense in that diminishes nickel dispersion. In Fig. 6 we can see reduction degree reached after activation stage. Reduction degree has been estimated comparing temperature programmed reduction curves corresponding to calcined and reduced sample. Reduction degree increases with nickel content. Finally, in Fig. 7 we can observe how active nickel area increases with nickel content until a certain value in which it begins to diminish.

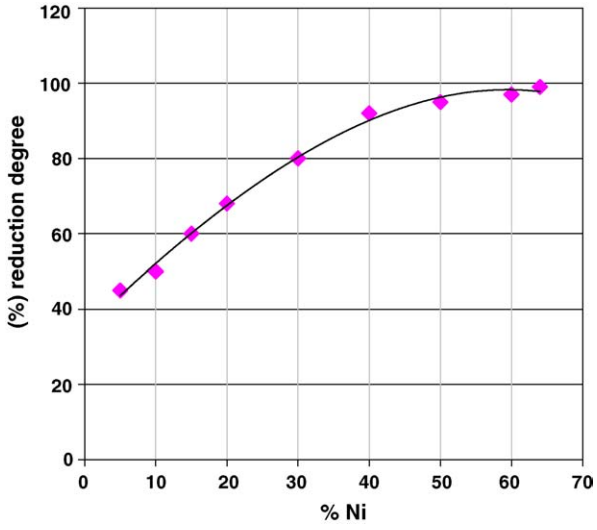

Fig. 6. Estimated reduction degree vs. nickel content.

3.2. Activation stage optimisation

Reaction conditions used to compare the conversion reached using HT-15 catalyst reduced on different ways, were $P = 10$ bar, $T = 723$ K, W/F = 2.5 g_{cat} h/hydrocarbon

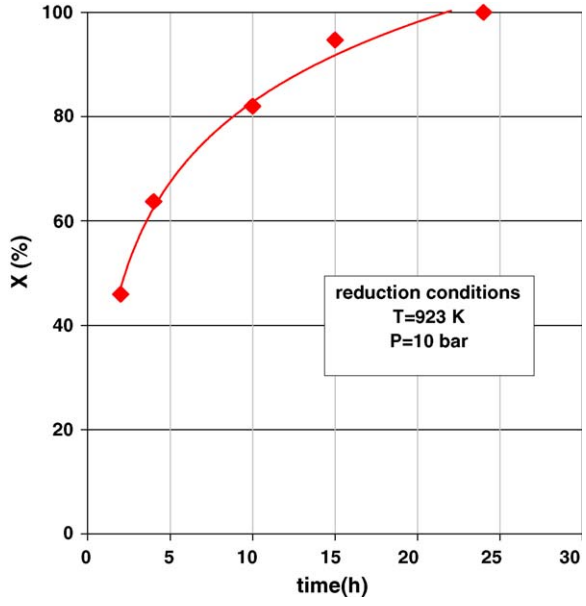

Fig. 8. Effect of reduction time on catalytic activity ($P = 10$ bar, $T = 723$ K, W/F = 2.5 g_{cat} h/hydrocarbon mol and S/C = $4H_2O$ mol/carbon atom).

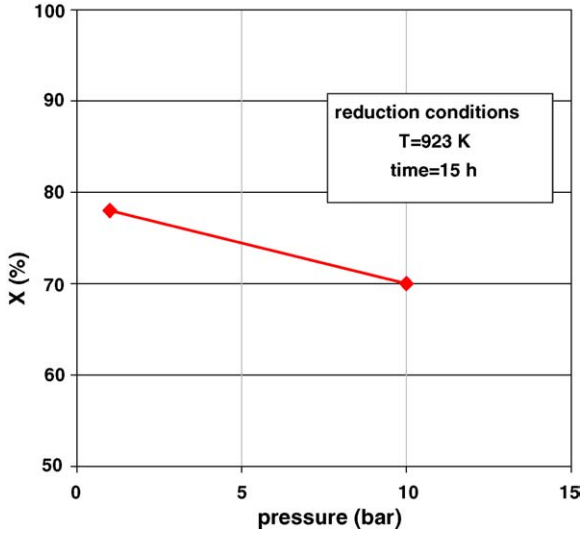

Fig. 9. Effect of reduction pressure on catalytic activity (P = 10 bar, T = 723 K, W/F = 2.5 g_{cat} h/hydrocarbon mol and S/C = 4H_2O mol/carbon atom).

mol and S/C = 4 H_2O mol/carbon atom; activation conditions have been indicated in Figs. 8–10. In order to determine optimal activation time, temperature and pressure have been maintained constant on several reduction tests, meanwhile activation process duration has been increased, in Fig. 8 we have represented conversion versus activation time. In this figure we can see the next: when reduction time increases from 15 to 24 h conversion increment is not significant, therefore activation process optimal duration will be 15 h. In order to determine optimal activation pressure two tests of reduction have been made, one at 10 bar and another one at atmospheric pressure, maintaining

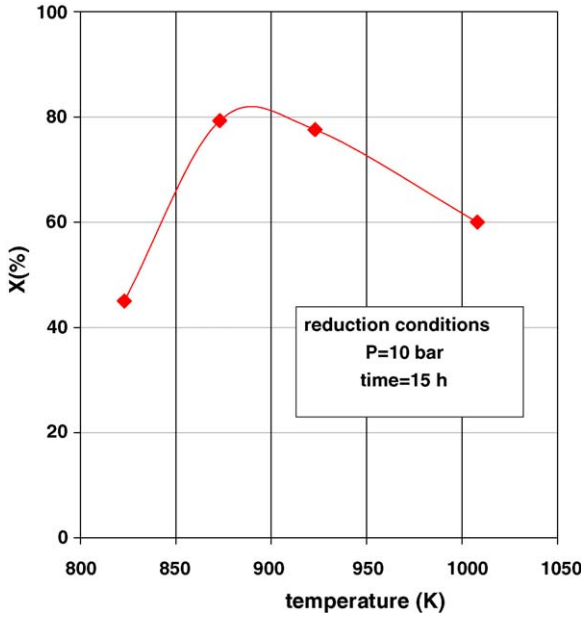

Fig. 10. Effect of reduction temperature on catalytic activity (P = 10 bar, T = 723 K, W/F = 2.5 g_{cat} h/hydrocarbon mol and S/C = 4H_2O mol/carbon atom).

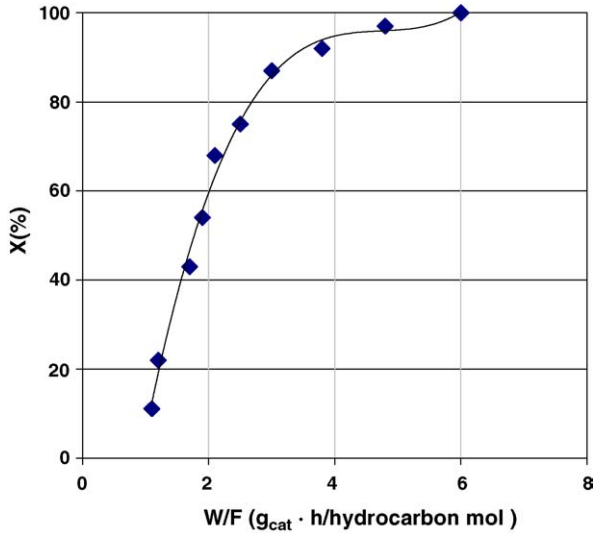

Fig. 11. Effect of contact time on hydrocarbon conversion ($P = P_{atm}$, T = 873 K, S/C = 3H_2O mol/carbon atom).

temperature and time constant; in Fig. 9 we can see how conversion obtained activating at atmospheric pressure is greater than the one obtained when activation process is carried out at 10 bar, therefore activation process optimal pressure will be atmospheric one. In order to determine optimal reduction temperature this variable has been changed. As can be seen in Fig. 10 temperature at which a higher conversion is reached was 873 K.

3.3. Effect of reaction conditions

For HT-15 catalyst, two series of tests have been made. First varying contact time and maintaining fixed rest of variables. As can be seen in Fig. 11 for short contact times hydrocarbon conversion is not total and gases produced

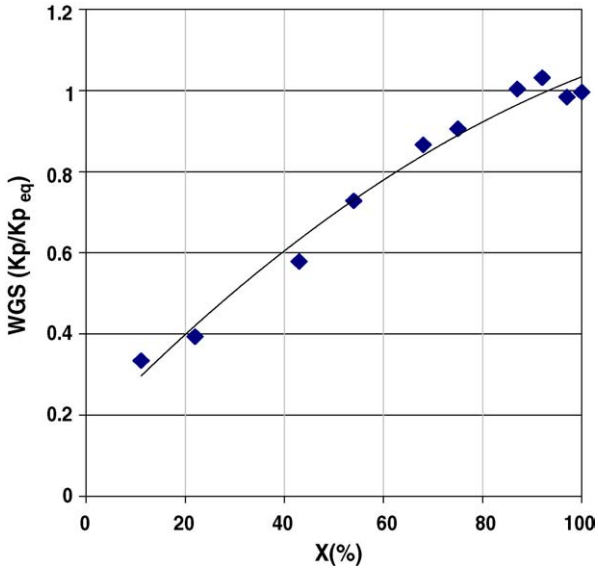

Fig. 12. Equilibrium of water gas shift reaction (WGS) ($P = P_{atm}$, T = 873 K, S/C = 3H_2O mol/carbon atom).

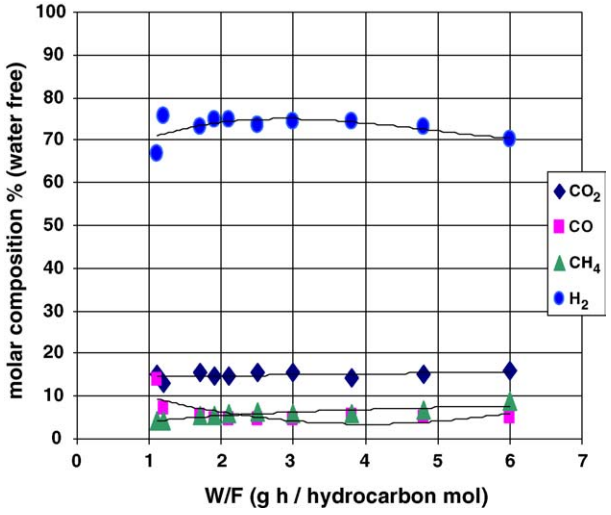

Fig. 13. Reaction product composition vs. contact time ($P = P_{atm}$, $T = 873$ K, S/C = 3H_2O mol/carbon atom).

during reaction do not reach thermodynamic equilibrium until a conversion higher than 80% is achieved (Fig. 12). In Fig. 13 we can see product distribution corresponding to different conversion level, in this figure we can see how hydrogen content decrease meanwhile methane content increase according to reaction (2).

Second series of tests has been made at a sufficiently great contact time to obtain total hydrocarbon conversion and to reach thermodynamic equilibrium of gases, thus we can study another variables influence (temperature, pressure and steam/carbon ratio) on reaction product composition. Higher hydrogen concentrations are obtained as temperature increases, pressure diminishes, and steam/carbon ratio increases (Fig. 14). It is necessary to indicate that working with a high steam/carbon ratio would give rise to a product in which hydrogen would be diluted by the excess of water, and thermal efficiency of the process would diminish.

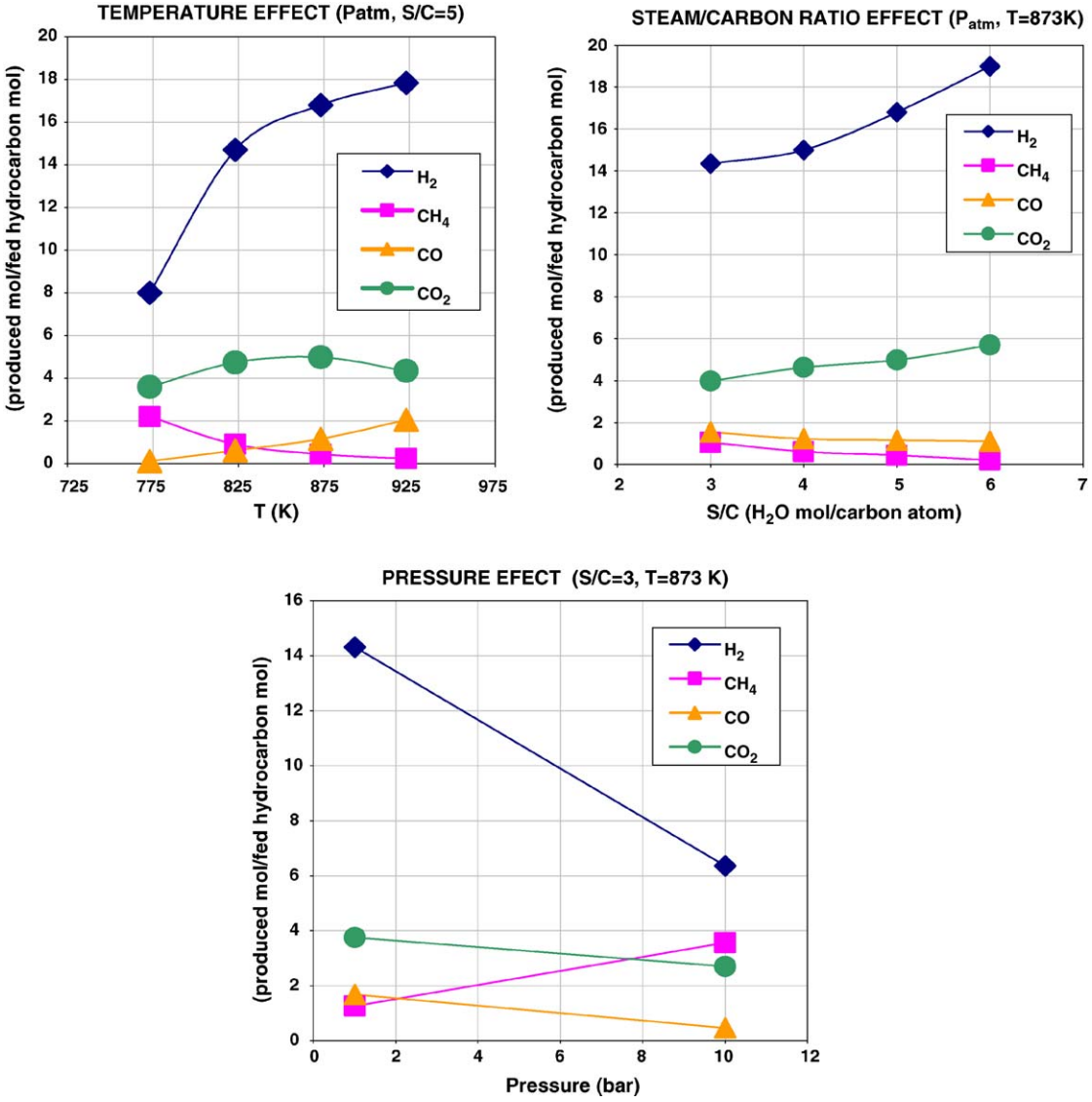

Fig. 14. Reaction product distribution based on operation conditions P, T and S/C (W/F = 8 g_{cat} h/hydrocarbon mol).

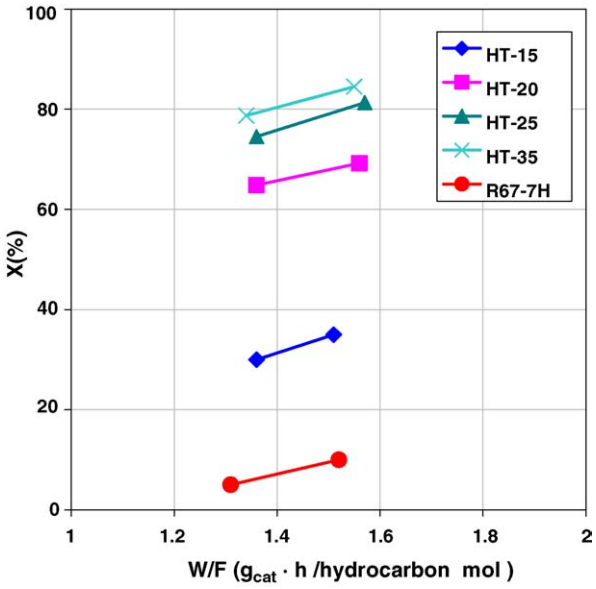

Fig. 15. Base catalyst activity (P = 10 bar, T = 723 K, S/C = 4H_2O mol/carbon atom).

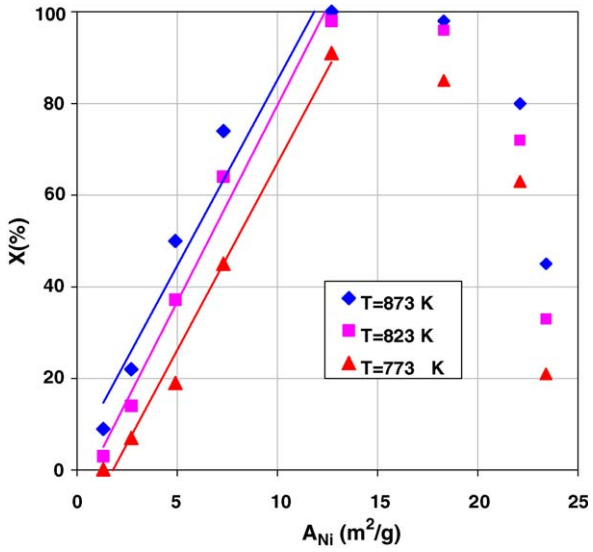

Fig. 17. Conversion vs. estimated active area ($P = P_{atm}$, W/F = 2 g_{cat} h/hydrocarbon mol, S/C = 3H_2O mol/carbon atom, T = 773–873 K).

3.4. Catalytic activity

A series of tests has been made to compare catalytic activity of several catalysts. Operation conditions are indicated in Fig. 15 in which we can see that all synthesized catalysts present greater conversion than the commercial one, with even equal or smaller nickel content. This is probably due to the high specific area that these catalysts present in which nickel is more dispersed than in the commercial catalyst.

We can see nickel content effect on catalytic activity in Figs. 16 and 17. In Fig. 16 we observe how activity increases as nickel content increases until nickel content is about 35 wt.%, then activity diminishes as nickel content increases. In Fig. 17 we have represented conversion versus estimated active area, in this figure we can see that a lineal relation exists until a nickel content of 30%, for greater nickel content, this relation is not lineal and, in spite of having greater nickel area, a diminution of the activity is observed. On catalysts with high nickel content, nickel is less dispersed and it presents greater particle size. On these catalysts could be possible that the combination of different textural properties (dispersion, form and size of crystals and superficial metallic planes proportion) could favour the

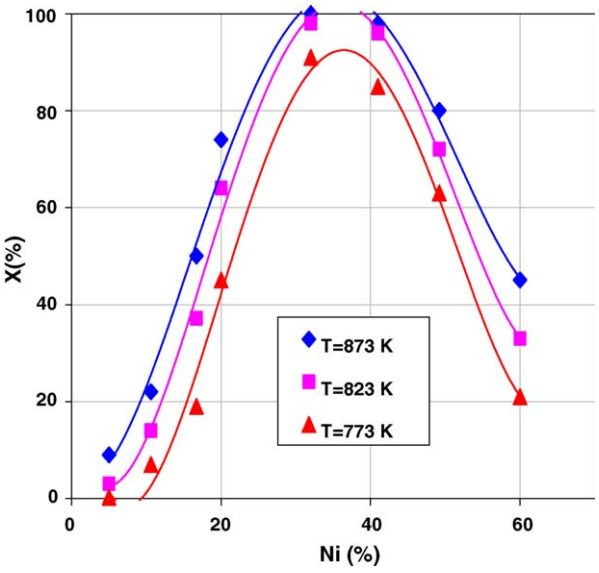

Fig. 16. Activity based on nickel content ($P = P_{atm}$, W/F = 2 g_{cat} h/hydrocarbon mol, S/C = 3H_2O mol/carbon atom, T = 773–873 K).

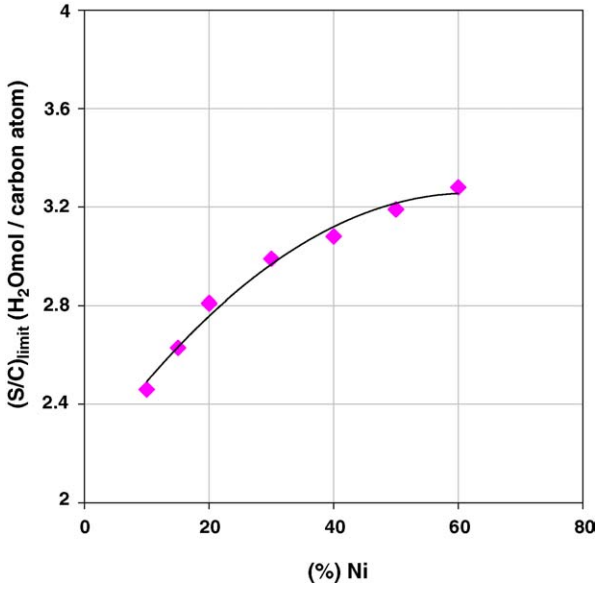

Fig. 18. Limit S/C ratio based on nickel content ($P = P_{atm}$, W/F = 8 g h/mol hydrocarbon, T = 823 K and $S/C_{initial}$ = 4H_2O mol/carbon atom).

reaction of C–C α-scission (reaction (5)) with respect to the recombination of C_1 species with oxygen species (reaction (7)). In this situation, concentration of C_1 species adsorbed on active sites would increase with time, being able to begin the process of nucleation of coke or coke precursors.

On the other hand, during catalysts manipulation we have observed that those that have higher nickel content, compact much worse than do those with lower nickel content. They also present less mechanical resistance and are susceptible to pulverize during process due to the high space velocity used; this could be other reason for anomalous results.

We can determine nickel content effect on resistance to carbon formation according to limit steam/carbon ratio, estimated by a relative manner. Operation conditions for this series of tests were: $P = P_{atm}$, W/F = 8 g_{cat} h/hydrocarbon mol, T = 823 K and $S/C_{initial} = 4H_2O$ mol/carbon atom.

In Fig. 18 we can see how limit steam/carbon ratio increases when nickel content decreases. This could be due to a larger dispersion and corresponding smaller nickel particle size of these catalysts. On catalysts with low nickel content, interaction with support will be greater than it is for catalysts with higher nickel content, and after activation stage, smaller nickel particles and greater dispersion are obtained. These properties could be the preferred ones to make that all C_1 species formed by C–C α-scission (reaction (5)) can be quickly gasified (reaction (7)). A small particle size and a high dispersion cause a diminution of the carbon formation rate, since it increases the induction period for the nucleation of carbon fibres [12]. In this reference also it is indicated that whichever minor is the size of nickel particle, minor is the steam concentration required at his around to assure complete gasification of adsorbed C_1 species.

In addition, resistance to carbon formation that show those catalysts with less nickel content also could be due to the greater magnesium content (see Fig. 1), that is a promoter used in commercial catalysts to reduce coke formation since it increases steam adsorption capacity (5). This variable, magnesium content, must be studied in the future.

4. Conclusions

Catalysts based on mixed oxides present greater catalytic activity and resistance to carbon formation in naphtha steam reforming reaction than do commercial catalyst. This is probably due to a high specific area of these catalysts, which permits higher nickel dispersion.

Catalytic activity increases as nickel content increases until approximately 30 wt.%, after that catalytic activity diminishes with nickel content. These results are related to metal dispersion and suitable combination of different textural properties.

Nickel content and temperatures of calcination and reduction stages, could be optimised to obtain a material which presents high catalytic activity and high resistance to carbon formation. Ideal situation would be that which combines all these variables to obtain a material with a suitable combination of textural properties (dispersion, form and metallic particle size, specific area and proportion of different superficial metallic planes) to get recombination of C_1 species with oxygen species coming from the water dissociation (reaction (7)) taking place at the same rate at which they have been formed from C–C α-scission (reaction (5)), and thus to avoid C_1 species remaining on active sites sufficient time to form coke.

Acknowledgements

We are thankful to the Generalitat Valenciana by its aid in the financing I + D (CTIDIB/2002/20) project. N. Morlanés thanks for to the Ministry of Science and Technology by the concession of a predoctoral scholarship (I3P/2001).

References

[1] Y.S. Seo, A. Shirley, S.T. Kolaczkowski, J. Power Sources 108 (2002) 213.
[2] M. Krumplet, R. Rumar, K.M. Myles, J. Power Sources 49 (1994) 37.
[3] R.A. Lemons, J. Power Sources 29 (1990) 251.
[4] Science Application International Corporation, Fuel Cell Handbook, fifth ed., National Technical Information Service, U.S. Springfield, VA, 2000.
[5] J.R. Anderson, M. Bouduart, Catalysis science and technology, in: J.R. Rostrup-Nielsen (Ed.), Catalytic Steam Reforming, vol. 5, Springer-Verlag editions, 1984 (Chapter 1).
[6] J.R. Rostrup Nielsen, J. Sehested, Adv. Catal. 47 (2002) 65.
[7] J.R. Rostrup Nielsen, Stud. Surf. Sci. Catal. 139 (2001) 1.
[8] J.R. Rostrup Nielsen, J. Catal. 209 (2002) 365.
[9] J. Sehested, A. Carlsson, T.V.W. Janssens, P.L. Hansen, A.K. Datye, J. Catal. 197 (2001) 200.
[10] J. Sehested, J.A.P. Gelten, I.N. Remediakis, H. Bengaard, J.K. Norskov, J. Catal. 223 (2004) 432.
[11] J. Ross, M. Steel, J. Catal. 52 (1978) 280.
[12] T. Borowieki, Appl. Catal. A: Gen. 4 (1982) 223.
[13] T. Borowieki, Appl. Catal. A: Gen. 4 (1984) 273.
[14] T. Borowieki, Appl. Catal. A: Gen. 4 (1987) 207.
[15] F. Arena, B.A. Horrell, D.L. Cocke, A. Parmaliana, N. Giordano, J. Catal. 132 (1991) 58.
[16] A. Parmaliana, F. Arena, F. Frusteri, S. Coluccia, L. Marchese, G. Martra, A.L. Chuvilin, J. Catal. 141 (1993) 34.
[17] F. Cavani, F. Trifiró, A. Vaccari, Catal. Today 11 (1991) 173.
[18] D. Tichit, B. Coq, Cattech 7 (2003) 206.
[19] A. Bhattacharyya, V.W. Chang, D.J. Schumacher, Appl. Clay Sci. 13 (1998) 317.
[20] M. Markevich, R. Coll, D. Montané, Ind. Eng. Chem. Res. 40 (2001) 4757.